1992

Influence of the Main Constructive Parameters of a Scroll Compressor on its Efficiency

R. Puff
Embraco S/A

M. Krueger
Embraco S/A

INFLUNCE OF THE MAIN CONSTRUCTIVE PARAMETERS OF A SCROLL COMPRESSOR ON ITS EFFICIENCY

Rinaldo Puff and Manfred Krueger
EMBRACO S/A - Research and Development
Rua Rui Barbosa 1020, Cx.P. D-27
Fax : 0055-474-412650
89200 - Joinville - SC - Brazil

ABSTRACT

This work presents an analysis of the influence of the main constructive parameters on the efficiency of a scroll compressor for air conditioner systems. A simulation program was developed and used as a designing tool. The program equations which computes the thermodynamic properties of gas, mass and energy losses and efficiency, are examined in detail. The program was validated comparing its results with experimental data from a compressor with capacity around 33,700 Btu/h. The parameters analyzed were: the number of compression chambers, the clearances and the characteristic dimensions of the pump. EER, capacity, power input and the individual efficiencies were obtained by varying each of the said parameters in the program data.

INTRODUCTION

A lot of effort has been spent in the search of new technologies for conservation and use of alternative energy sources. In refrigeration and air conditioning area, new types of compression mechanisms have been developed in order to reduce the energy consumption by the increase of the efficiency. One of these compression mechanisms is the scroll compressor.

The scroll compressor has shown the following advantages over reciprocating and other rotaries, in high back pressure condition:

- Higher specific capacity due to lower leakages and no back flow and dead volume losses.
- Lower consumption due to absence of valves and lower friction power losses.
- Lower noise levels, due to lower pressure gradients.
- Higher motor efficiency, due to lower starting needs.
- Until 20% reduction in weight and size, when compared with conventional reciprocating compressors.

The objective of this work is to analyze the influence of the main constructive parameters on the scroll compressor efficiency. A simulation program is used as an analyzing tool. The model is based on the simulation of the full compression cicle, which depends on the number of compression chambers considered. Polytropic compression is considered in order to compute the thermodynamic properties of the gas into the compression chambers. The simulation program was validated comparing its results with experimental data from a compressor with capacity of 33,700 Btu/h. The curves of pressure, temperature and mass as function of the shaft position are presented.

NUMERICAL MODEL

Compression Cicle Simulation

The numerical simulation is done solving a set of equations simultaneously for each of the "n" chambers considered. The volume of the chambers as function of the shaft position are computed using the equations obtained in Ref. 01. A mass balance is done at every shaft position, in order to find the mass of refrigerant into the chambers. The thermodynamic properties of the gas, like pressure, temperature and specific volume, are computed using a polytropic model as shown below.

Suction process: Constant gas properties are considered.

$$\rho i(\Theta) = \rho s \tag{01}$$

$$Pi(\Theta) = Ps \tag{02}$$

$$Ti(\Theta) = Ts \tag{03}$$

Compression and discharge process: Properties vary with the shaft position

$$\rho i(\Theta) = \frac{Mi(\Theta)}{Vi(\Theta)} \tag{04}$$

$$Pi(\Theta) = Ps \cdot \left[\frac{Mi(\Theta)}{\rho s . Vi(\Theta)} \right]^{kn} \tag{05}$$

$$Ti(\Theta) = Ts \cdot \left[\frac{Pi(\Theta)}{Ps} \right]^{(kn-1)/kn} \tag{06}$$

Suction	Compression	Discharge
$i = n;\ 0 < \Theta < 2\Pi$	$i > 2;\ 0 < \Theta < 2\Pi$ $i = 2;\ 0 < \Theta < \Theta a$	$i = 2;\ \Theta a < \Theta < 2\Pi$ $i = 1;\ 0 < \Theta < \Theta a$

Mass Flow Losses

There are three kinds of mass losses that occur in a scroll compressor. When the gas comes into the suction shell, heat is transferred to it by the internal walls, which are in a higher temperature. This increasing of the suction gas temperature reduces its specific volume and the amount of gas that is really suctioned by the scroll orbiting movement is lower. The suction heating loss is than given by:

$$\dot{M}hl = \dot{M}a \cdot \left(\frac{\rho ls}{\rho s} - 1 \right) \tag{05}$$

Once into the compression chambers, there is a pressure difference between each chamber and the next one. Due to that, gas leaks through the top and flank clearances. The leakage between the "n-1" and "n" volumes consists in a mass loss. Both are calculated with the general equation of isentropic flow through a convergent-divergent nozzle.

$$Mlk = \phi t.At.C + \phi f.Af.C \tag{06}$$

where:

$$C = (Pu + Pdo) \cdot \sqrt{\frac{2.k}{G.(Tu+Tdo)} \cdot \left[\frac{2}{(k+1)} \right]^{(k+1)/(k-1)}} \tag{07}$$

$$At = \delta t.\Pi.\{a.[2\Pi.(n-i+1) + (\Pi-\Theta)] - th/2\} \tag{08}$$

$$Af = \delta f.h/2 \tag{09}$$

ϕt and ϕf are reduction coefficients due to the presence of oil sealing the clearances. The third gas losing way is by the mixture with lubricating oil. It is not computed by the program due to the assumption that in this compressor this mass flow loss is much lower in comparison to the others.

Energy Losses

In Figure 01 we can see the energy diagram for a scroll compressor. The compressor input power (Ein) is given by the summation of the theoretical power (Wth) with the energy losses that occur during the compressor running.

$$\dot{E}in = \dot{W}th + \dot{E}ml + \dot{E}fl + \dot{E}oc + \dot{E}th \qquad (10)$$

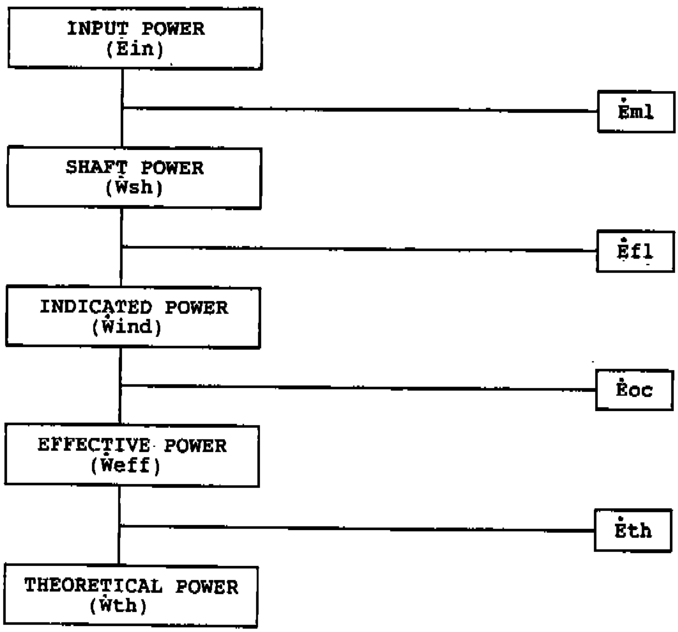

Figure 01. Energy Diagram

The theoretical power is the ideal work necessary to compress the gas from the suction pressure (Ps) to the discharge pressure (Pd). It is given by the following equation.

$$\dot{W}th = \frac{k}{(k-1)} \cdot \frac{Ps.Ma}{\rho s} \cdot \left[\left(\frac{Pd}{Ps} \right)^{(k-1)/k} - 1 \right] \qquad (11)$$

or,

$$\dot{W}th = \dot{M}a \cdot (hd - hs) \qquad (12)$$

The electrical motor losses occur due to the cooper and iron losses. There is a low variation of these, due to the variation of the motor temperature. As this variation is very low, we may consider the losses being constants. We may also admit as constant the motor efficiency (ηMot), considering steady-state running conditions. Then the motor losses become:

$$\dot{E}ml = \dot{E}in \cdot (1 - \eta Mot) \qquad (13)$$

The mechanical losses occur due to the friction caused by the relative movement between the moving parts of the compressor.

$$\dot{E}bg = \mu o.2\Pi.\omega^2.\left[\frac{Lb1.Rb1^3}{\delta b1} + \frac{Lb2.Rb2^3}{\delta b2} + \frac{Lbe.Rbe^3}{\delta be} \right] \tag{14}$$

$$\dot{E}thr = f \;.\; Wrot \;.\; Rthr \;.\; \omega \tag{15}$$

$$\dot{E}os = \frac{\mu o.Aos.2\Pi.e.\omega^2}{\delta t} \tag{16}$$

where,

$$Aos = a/2.\{[\ \Pi.(2n-1)]^2 - \Theta a^2\ \} \tag{17}$$

$$\dot{E}or = 4.\mu o.(4.e.\omega c)^2 \;.\; \left(\frac{Aor1}{\delta k} + \frac{Aor2}{4\delta or} \right) \tag{18}$$

where,

$$Aor1 = 2.hk.bk \qquad ; \qquad Aor2 = \Pi.bk.(2Ror - bk) \tag{19}$$

$$\dot{E}fl = \dot{E}bg + \dot{E}thr + \dot{E}os + \dot{E}or \tag{20}$$

Where Ebg are the bearings losses, Ethr are thrust bearing losses, Eos are the orbiting scroll losses and Eor are the oldham ring losses.

Analyzing the P-V diagram in Figure 02, We can see that the area "A" is the indicated power. This one is the power really used to compress the gas. It is computed by integration during the compression cicle.

$$\dot{W}ind = \omega \;.\; \oint \sum_{i=1}^{n} (Pi(\Theta)-Ps).dV \tag{21}$$

area "B" shows the over compression losses, which occur when the pressure inside each compression chamber overcomes the discharge pressure. They are obtained as below.

$$\dot{E}oc = \omega \;.\; \oint \sum_{i=1}^{n} (Pi(\Theta) - Pd).dV \qquad \text{if } Pi(\Theta) > Pd \tag{22}$$

The effective power is given by the indicated power minus the over compression losses. The area "C" shows the thermodynamic losses, which are resultant from the gas heating during the compression process. They are given by the difference between the effective and the theoretical power.

$$\dot{W}ef = \dot{W}ind - \dot{E}oc \tag{23}$$

$$\dot{E}th = \dot{W}ef - \dot{W}th \tag{24}$$

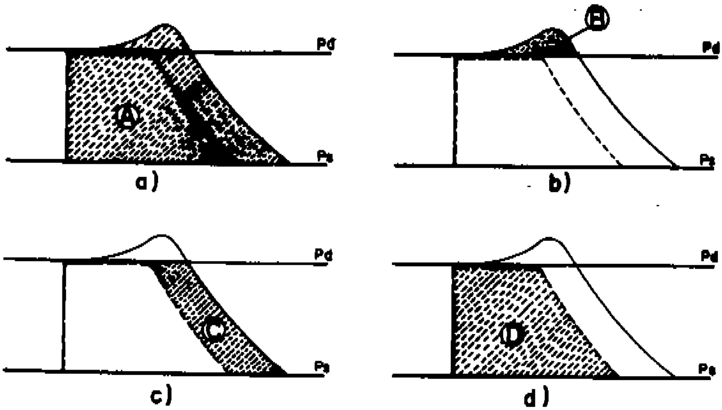

Figure 02. The P-V diagram

Efficiency

To evaluate the efficiency of the compressor, we use the development done by P. Pandeia and W. Soedel, shown in Ref. 02. An efficient compressor is that which can pump the maximum mass of gas with the minimum energy consumption. Then it is possible to obtain two performance criteria:

1. Capacity, which is the mass flow that can be pumped. A higher mass flow represents a higher performance.
2. Consumption, which is the power input needed to pump the gas. A higher consumption decreases the performance.

In a mathematic scheme they becomes:

1. Performance $\propto$ Capacity
2. Performance $\propto$ 1 / Consumption
3. Performance $\propto$ Capacity / Consumption

With that we can now define the EER (Energy Efficiency Ratio) as being the ratio between the frigorific capacity and the energy consumption.

$$EER = \frac{\dot{M}a . \Delta He}{\dot{E}in} \tag{25}$$

We can also define another term, performance ratio (Π) to remove the proportionality sign.

$$\Pi = \frac{(\partial m/\partial t)}{(\partial Ein/\partial m)} = \frac{(\partial m/\partial t)^2}{(\partial Ein/\partial t)} \tag{26}$$

The performance ratio as shown above is an adimensional term. Due to that, it does not show the better possibility of performance. We can then define another term called performance efficiency (ηp), which is obtained comparing the real performance ratio with the ideal one.

$$\Pi a = \frac{(\partial m/\partial t)a^2}{(\partial Ein/\partial t)} \quad ; \quad \Pi i = \frac{(\partial m/\partial t)i^2}{Eid} \tag{27}$$

$$\eta p = \frac{\Pi a}{\Pi i} = \frac{(\partial m/\partial t)a^2}{(\partial Ein/\partial t)a} \cdot \frac{Eid}{(\partial m/\partial t)i} \tag{28}$$

$$\eta p = \frac{(\partial m/\partial t)a}{(\partial m/\partial t)i} \cdot \frac{(\partial m/\partial t)a.Eid}{(\partial Ein/\partial t)a} \tag{29}$$

$$\eta p = \eta Ma \,.\, \eta e \tag{30}$$

We can also write ηp as being:

$$\eta p = \frac{(\partial m/\partial t)a}{(\partial m/\partial t)i} \cdot \frac{(\partial m/\partial t)a.Ere}{(\partial Wsh/\partial t)} \cdot \frac{Eid}{Ere} \cdot \frac{(\partial Wsh/\partial t)}{(\partial Ein/\partial t)a} \tag{31}$$

$$\eta p = \frac{\dot{M}a}{\dot{M}i} \cdot \frac{\dot{M}a.Ere}{\dot{W}sh} \cdot \frac{Eid}{Ere} \cdot \frac{\dot{W}sh}{\dot{E}in} \tag{32}$$

Finally,

$$\eta p = \eta Ma \,.\, \eta Mec \,.\, \eta Th \,.\, \eta Mot \tag{33}$$

Were, Eid and Ere are the ideal and real specific work, respectively

PROGRAM VALIDATION

To prove the suitability of the program, we will show in this topic the results obtained from its use. It is considered a compressor with three compression and a suction chamber, totalyzing four, working simultaneously. The refrigerating gas used is the HCFC-22, normaly used in air conditioners. The running conditions are shown in Table 01.

In Figure 03 we can see the pressure X θ chart for the four chambers. We can observe the pressure picks formed into the compression pockets before they open to the discharge side. We are using a constant suction pressure during the suction process, because it is considered a steady-state process.

Evap. Temperature	7.2 C	Cond. Temperature	54.4 C
Amb. Temperature	35.0 C	Super heating	35.0 C
Sub cooling	46.1 C	Suc. Temperature	55.0 C
Frequency	60.0 Hz	ηMot	83.0 %

Table 01. Running conditions

Figure 04 shows the variation of the gas temperature during the compression. As a polytropic compression is considered, the behavior of the temperature is similar to the pressure. A more accurate first law model could give better results, but for our proposes it is sufficient.

A mass X θ chart is shown in Figure 05. We can observe that in each chamber, there is an increasing of the mass before it opens to the discharge side. It occurs due to the leakage comming from the next chamber. The discharge process is very stable, because there is no discharge valve required in this kind of compressor as explained before.

The comparison between experimental data and the results obtained with the developed program is shown in Table 02. In the bar chart of Figure 06 we can see the comparison between the individual efficiencies of the compressor.

	SIMULATION	EXPERIMENTAL
Displ. [cc/rev]	43.4	43.4
Capacity [Btu/h]	31,000	33,700
Consumption [W]	3,160	3,300
EER [Btu/Wh]	9.80	10.30

Table 02. Results comparison

CONSTRUCTIVE PARAMETERS ANALYSIS

Variation of the Number of Compression Chambers

Increasing the number of compression chambers and computing the other dimensions like the generation radius, wall thickness and scroll height in order to keep constant the displacement of the compressor, we shall get the curves shown in Figure 07. It shows the variation of the individual compressor efficiencies. We can observe that mechanical and mass efficiencies are almost constant. The mayor difference is observed in the thermodynamic efficiency. It decreases with the increasing of "n", due to the higher over compression losses. The compressed gas overcomes the discharge pressure earlier and is maintained more time over compressed, increasing the thermodynamical losses, and consequently reducing efficiency.

Variation of the Tip and Flank Clearances

Varying the tip and flank clearances and keeping constant all the other parameters, we shall get the chart shown in Figures 08 and 09. With the increase of the clearances, we have an increasing of the mass comming in each chamber due to the leakage from the next one, and it decreases the mass efficiency. We have also a reduction in the thermodynamical efficiency due to the compression of the leaked gas.

Variation of the Principal Dimensions

The variation of the compressor principal dimensions is done keeping constant its displacement. The result of this variation is shown in Figure 10. It is observed that we have an optimum generation radius for this compressor. Lower values for this dimension increase so much the scroll height, increasing the flank leakage and reducing mass efficiency. Greather values aren't advantageous too, because the increase of the generating radius increases the external scroll diameter and the eccentricity. That increases the friction area between the scrolls, increasing the mechanical losses and decreasing the mechanical efficiency.

FINAL COMMENTS

The influence of the main constructive parameters on the efficiency of a scroll compressor was presented. The analysis was made over charts, which showed each compressor efficiency separately. This gives a clear idea of how the changes in performance occur. For example, we observed that in a scroll compressor, the increasing of the number of compression chambers decreases the thermodynamical efficiency, because the gas is maintained more time over compressed during the compression cicle. The variation of the clearances affect directly the mass efficiency due to the increasing of the leakage from each chamber to its adjacent with lower pressure. This forces the gas to stay more time being compressed, decreasing the compressor thermodynamic efficiency too. The influence of the principal dimensions is shown too. There is an optimum value for the generation radius. If we take lower values for it, there is an incresing of the scroll height, increasing the flank leakage and reducing the compressor mass efficiency. On the other hand, higher values increase so much the external scroll radius and the eccentricity, increasing the friction area, and reducing the mechanical efficiency. Therefor any "a" value out of the range, affect negatively the overall compressor efficiency (EER).

The simulation program used, in spite of a simplified compression model, gave satisfactory results. The calculation of the gas thermodynamic properties simultaneously for each compression chamber proved to bee important for the simulation scheme.

SYMBOLS

n	- Number of chambers;
a	- Generating radius;
th	- Wall thickness;
e	- Eccentricity;
θ	- Shaft position angle;
θa	- Discharge begining angle;
kn	- Polytropic index;
k	- Cp / Cv;
G	- Refrigerant constant;
$Mi(\theta)$	- Mass of gas into the i chamber;
$Pi(\theta)$	- Gas pressure into the i chamber;
$Ti(\theta)$	- Gas temperature into the i chamber;
$\rho i(\theta)$	- Specific mass of the gas into the i chamber;
$Vi(\theta)$	- Volume of the i chamber;
Pd	- Discharge pressure;
hd	- Discharge gas enthalpy;
Ts	- Suction Temperature;
Ps	- Suction pressure;
hs	- suction gas enthalpy;
ρs	- Suction gas specific mass;
ρls	- Suction line gas specific mass;
μo	- Oil viscosity;
f	- Friction coeficient;
ω	- Running frequency;
ωc	- Shaft angular velocity;
Lb1, Lb2, Lbe	- Bearings lenght;
Rb1, Rb2, Rbe	- Bearings Radius;
$\delta b1$, $\delta b2$, δbe	- Bearings clearances;
Wrot	- Rotor weight;
Rthr	- Thrust bearing radius;
hk, bk	- Key height and lenght;
δk	- Key clearance
δor	- Oldham ring clearances
Ror	- Oldham ring external radius

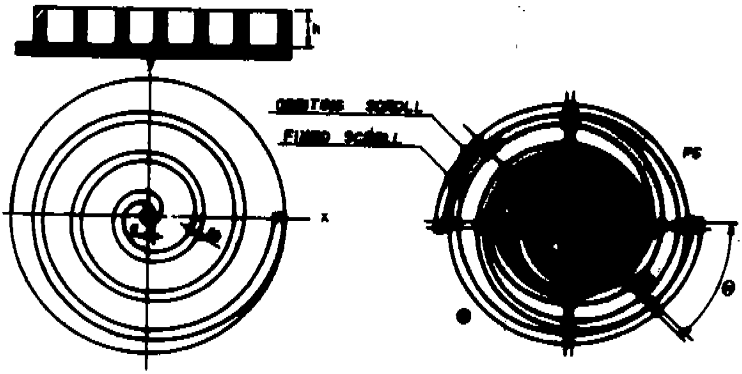

Figure 11. Scroll geometry.

REFERENCES

[01] Morishita, E., Sugihara, M., Inaba, T., Nakamura T., Scroll Compressor Analytical Model. Mitsubishi Eletric Corporation, Japan.

[02] Pandeya, P.N., Soedel, W., A Generalized Approach Towards Compressor Performance Analysis. Purdue Compressor Technology Conference, 1978.

[03] Uchikawa, N., Terada, H., Arata, T., Scroll Compressors For Air Conditioners. Hitachi Review, Vol. 36, No. 3, 1987.

[04] Morishita, E., Sugihara, M., Nakamura, T., Scroll Compressor Dynamics. Bulletin of JSME, Vol. 29, No. 248, February 1986.

[05] Fuller, D.D., Theory and Practice of Lubrication for Engineers. John Wiley & Sons, N.Y., 1984.

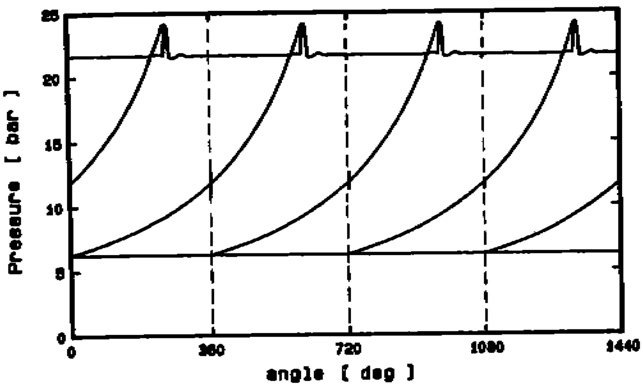

Figure 03. Pressure X θ.

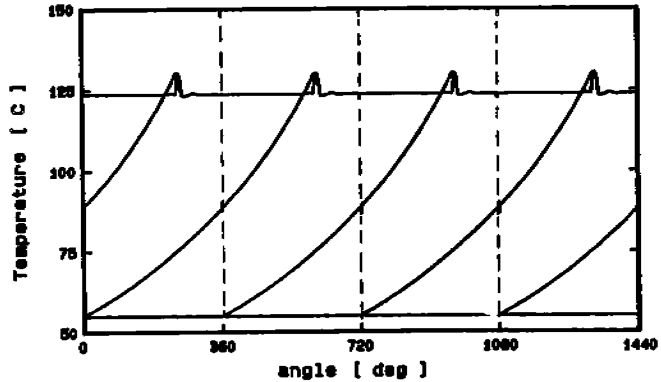

Figure 04. Temperature X θ

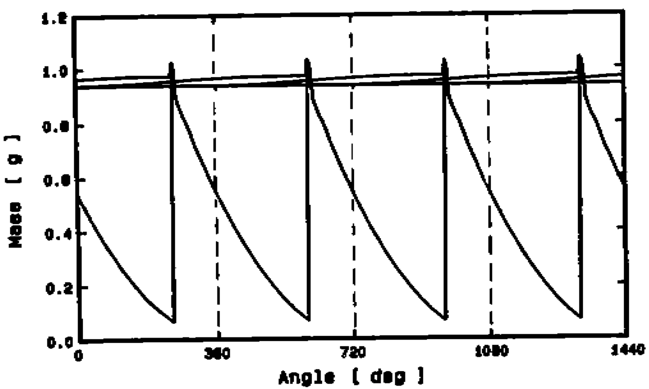

Figure 05. Mass X θ

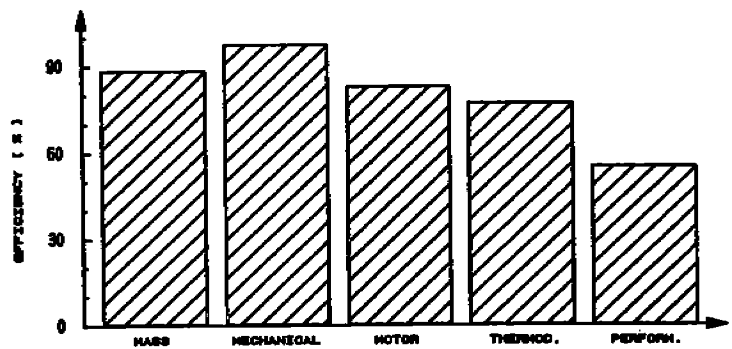

Figure 06. Individual efficiencies.

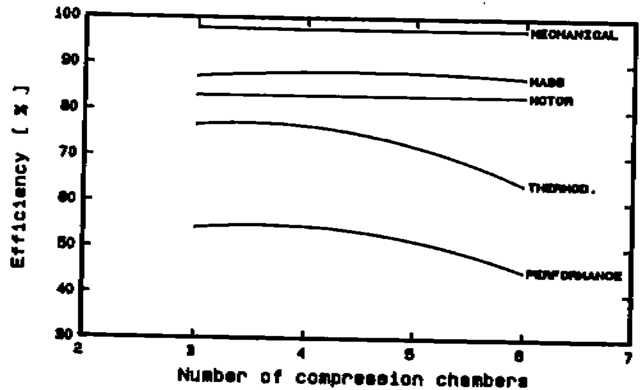

Figure 07. Efficiencies X Number of compression chambers

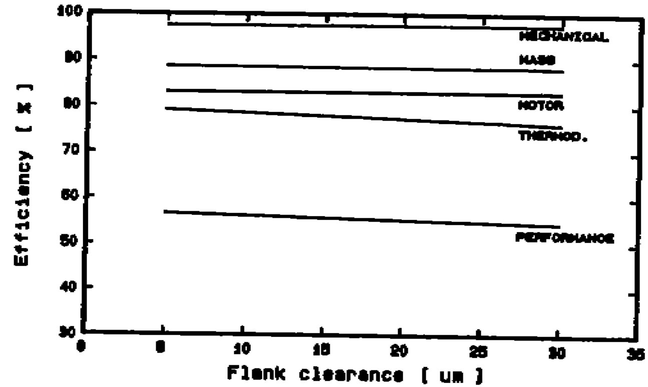

Figure 09. Efficiencies X Flank clearance

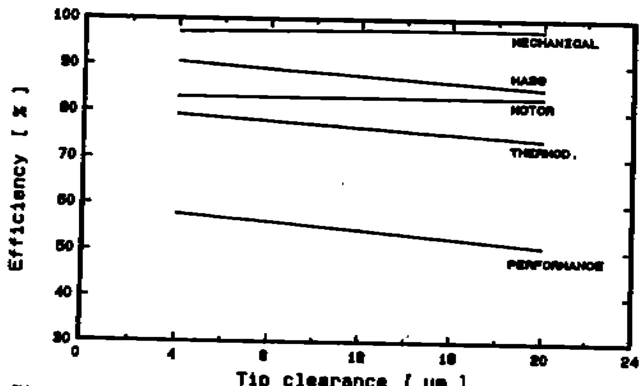

Figure 08. Efficiencies X Tip clearance

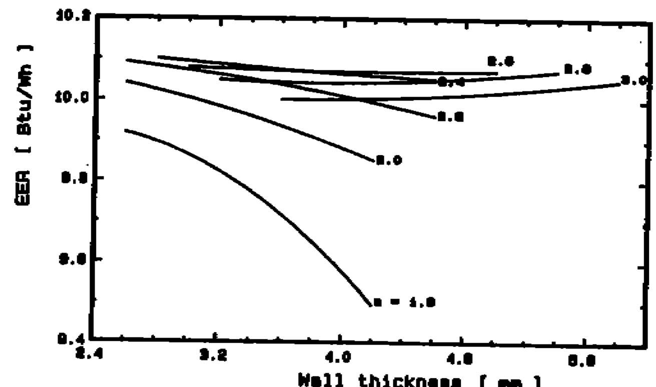

Figure 10. EER X Principal dimensions variation